J Biol Phys (2006) 32:507–521
DOI 10.1007/s10867-007-9033-4

RESEARCH PAPER

Computational Phlebology: The Simulation of a Vein Valve

Gavin A. Buxton · Nigel Clarke

Received: 25 September 2006 / Accepted: 10 January 2007 /
Published online: 13 February 2007

Abstract We present a three-dimensional computer simulation of the dynamics of a vein valve. In particular, we couple the solid mechanics of the vein wall and valve leaflets with the fluid dynamics of the blood flow in the valve. Our model captures the unidirectional nature of blood flow in vein valves; blood is allowed to flow proximally back to the heart, while retrograde blood flow is prohibited through the occlusion of the vein by the valve cusps. Furthermore, we investigate the dynamics of the valve opening area and the blood flow rate through the valve, gaining new insights into the physics of vein valve operation. It is anticipated that through computer simulations we can help raise our understanding of venous hemodynamics and various forms of venous dysfunction.

Key words vein valves · phlebology · venous · simulation · lattice spring model · lattice Boltzmann

1 Introduction

Veins are vessels which return de-oxygenated blood to the heart. The mechanism by which this occurs is through a "peripheral heart" system consisting of veins, their valves and the surrounding leg muscles [1, 2]. During muscular contraction, the vein vessels are locally squeezed by the surrounding leg muscles. This results in a pressure gradient which would cause blood to flow in both directions, but for the presence of vein valves. The valves are composed of two intraluminal membranous structures, or valve cusps, and ensure that blood only flows proximally back to the heart [1, 2]. In particular, the valve cusps meet in the centre of the vein vessel and prevent retrograde (proximal to distal) blood flow by occluding the vessel. Blood

G. A. Buxton (✉) · N. Clarke
Department of Chemistry, University of Durham, Durham, DH1 3LE, UK
e-mail: g.a.buxton@durham.ac.uk

circulation through veins depends upon the unidirectional nature of vein valves and their dysfunction, in this regard, causes almost all known venous disorders [3].

Venous diseases are common and can be debilitating or even fatal [4]. Venous dysfunction allows retrograde blood flow in the veins which is detrimental to circulation and can result in stagnation and blood clots. There are a number of reasons why venous reflux can occur. In some patients, the valve cusps have been observed to attach to the vein wall in such a way as to leave an intermediary gap [5]. That is, the valve cusps no longer meet in the centre of the vein and a reversal of the pressure gradient (resulting in retrograde flow) is required to bring these cusps together and occlude the vessel. Venous dysfunction can arise as a consequence of valve failure, where the valve cusps become shrunken, deformed, or perforated and, therefore, incompetent [6]. Normal valve leaflets, however, are mechanically robust, and the valve cusps are more than capable of withstanding the physiological stresses imposed by the blood flow [7]. Venous dysfunction can also develop through venous dilation [3]. In other words, the vein walls become increasingly stretched such that the valve cusps are pulled apart and no longer meet in the centre of vein. Retrograde blood flow can, therefore, occur through this opening and through the vein valve. It is believed that a better understanding of venous hemodynamics will give crucial insights into these conditions.

It was previously thought that venous valves closed only in response to a sufficiently large reverse flow velocity [8]. This is no longer thought to be the case, and the vein valves are now thought to respond to pressure gradients [9]. Significant insights into the physics of vein valves have been obtained through recent developments in ultrasound technology by Lurie et al. [10–12]. They have been capable of visualising in situ both the vein valve cusps and the blood flow through the valve. This led to the characterisation of four phases to the valve cycle: opening, equilibrium, closing and closed [12]. Interesting dynamic behaviour was observed during the equilibrium phase (when the valve is fully opened). The leading edges of the valve cusps were observed to flutter as the blood streamed past (much as a flag flutters in the wind) and vortical flow was observed behind the valve cusps in the valve sinuses [11]. It is this complex interaction between venous hemodynamics and valve solid mechanics that make modelling vein valves challenging.

Vein valves have been ‘modelled’ experimentally. That is, an artificial system which mimicked vein valves was constructed from latex tubing and polyurethane film [5]. This approach allowed the systematic investigation of valve geometry without having to account for physical variations in vein valves that occur naturally from one individual to the next. However, to the best of our knowledge, there has been no computer modelling work on the fluid–structure interactions in vein valves reported in the literature. We have, therefore, developed a simple fluid–structure interaction model which captures the qualitative behaviour of vein valves.

The fluid in our model is captured using a lattice Boltzmann (LB) model, while the solid mechanics is captured using a lattice spring model (LSM). The LB method and LSM are both computationally efficient models whose local rules are guided by atomistic phenomena, but whose emergent behaviour captures the continuum physics of the problem. In particular, the LB technique proceeds through the propagation and collision of fluid distributions on a simple lattice, similar to the propagation and collision of fluid atoms on the microscopic scale [13]. In a similar manner, the LSM consists of a lattice of interconnected springs and is adopted from

solid state physics and early atomistic models which considered harmonic interatomic potentials [14]. The LB model and the LSM can be shown to recover the desired Navier–Stokes equation and continuum elasticity theory, respectively.

These models have previously been coupled in order to capture the dynamics of a microcapsule impacting on either a hard or sticky surface [21]. Here, we extend the approach to capture the two-dimensional nature of both the valve cusps and the vein walls and apply our dynamic three-dimensional model to the simulation of vein valve structures. We give details of this computational technique in the following section. Results and discussion are presented in Section 3. Finally, we summarise our results and draw relevant conclusions in Section 4.

2 Methodology

2.1 Solid Mechanics

In order to simulate the elastic mechanics of the vein wall and the vein valves, we use the lattice spring model (LSM). While the solid regions of the vein walls and the vein valve are three-dimensional, we capture the physics of the deformation of these solid regions using a two-dimensional LSM. In other words, we treat both the vein wall and the valves as elastic membranes which can freely bend and take into consideration stretching forces only. This is reasonable for very thin shells, but may not be reasonable for vein walls which may exhibit bending effects, nonlinear behaviour and anisotropy. The continuum elastic membrane is replaced by a discrete set of elastic springs connecting regularly spaced nodal points. The elastic energy at node i can be given by [14]

$$A_i = \frac{1}{2}\sum_j k_{ij}\left(|\mathbf{r}_{ij}| - |\mathbf{r}^0_{ij}|\right)^2 \tag{1}$$

where the summation is over all nearest- [10] and next-nearest- [11] neighbouring nodes of a simple square lattice. The difference between the position of node i and the neighbouring node j is $\mathbf{r}_{ij}$, and the equilibrium distance is $\mathbf{r}^0_{ij}$. We consider simple Hookean springs where k_{ij} is the spring constant. This form of the free energy can be linearised and mapped onto continuum elasticity theory to give the following in-plane Young's modulus [14, 15]

$$Eh = \frac{8kh}{3\Delta x} \tag{2}$$

where the thickness of the vein wall is given by h, k is a force constant and Δx is the equilibrium unit length of the LSM lattice. The Poisson's ratio (defined as the ratio of transverse contraction strain to longitudinal extension strain) is fixed at $\frac{1}{3}$ in the absence of non-central interactions.

The elastic forces that act on the nodal points can be obtained from the derivative of the free energy. The force acting on node i due to the deformation of the spring between nodes i and j is given by

$$F_{ij} = -\frac{\partial A_i}{\partial \mathbf{r}_{ij}} = -k_{ij}\left(\frac{|\mathbf{r}_{ij}| - |\mathbf{r}^0_{ij}|}{|\mathbf{r}_{ij}|}\right)\mathbf{r}_{ij}. \tag{3}$$

Given the forces acting on the nodal points, we can update the nodal positions. To capture the dynamics of this system, we assign masses to the nodal points and integrate Newton's equation of motion,

$$\mathbf{F}_i = M_i \frac{\partial^2 \mathbf{r}_i}{\partial t^2} \tag{4}$$

where M_i is the mass at node i and $\mathbf{F}_i$ the force acting on this mass. Newton's equation of motion can be integrated using the velocity Verlet algorithm [16]. This allows us to obtain the velocity at the nodes and, when coupling the solid and fluid systems, transfer the velocities at the bounding solid walls to the enclosed fluid. The velocity Verlet algorithm updates the position, velocity and acceleration of the nodal masses in the following manner [16],

$$\begin{aligned}
\mathbf{r}_i\left(t+\Delta t\right) &= \mathbf{r}_i\left(t\right) + \mathbf{v}_i\left(t\right)\Delta t + \frac{1}{2}\mathbf{a}_i\left(t\right)\Delta t^2 \\
\mathbf{v}_i\left(t+\frac{\Delta t}{2}\right) &= \mathbf{v}_i\left(t\right) + \frac{1}{2}\mathbf{a}_i\left(t\right)\Delta t \\
\mathbf{a}_i\left(t+\Delta t\right) &= \frac{\mathbf{F}_i\left(t\right)}{M_i} - D_i\mathbf{v}_i\left(t+\frac{\Delta t}{2}\right) \\
\mathbf{v}_i\left(t+\Delta t\right) &= \mathbf{v}_i\left(t+\frac{\Delta t}{2}\right) + \frac{1}{2}\mathbf{a}_i\left(t+\Delta t\right)\Delta t
\end{aligned} \tag{5}$$

where $\mathbf{v}_i$ and $\mathbf{a}_i$ are the velocity and acceleration of node i, respectively. The damping constant, D_i, dampens internal elastic waves. In this manner, we can dynamically evolve the mechanics of the vein walls and valve structure subject to external (fluid pressure) and internal (elastic) forces.

The elastic shells which make up both the vein walls and vein valves in our model are considered to be 2D elastic films which are curved. The vein wall is assumed to be cylindrical in shape and the 2D LSM lattice is wrapped around to form the cylinder. The vein valves are created from sections of ellipsoidal tubes to give an appropriate curvature to the valves. The valves intersect at right angles with the vein walls at the base of the valve sinus while at the centre of the channel the valves meet and the valve walls run parallel with the vein walls. This geometry is depicted in Fig. 1, which shows the lattices for the two valves (labelled a and b) and the vein wall (labelled c) both collectively and, for clarity, separately. By changing the aspect ratio of the ellipsoidal geometry of the vein valves, we can specify the sinus depth of the valves. Regions in the vein wall surrounding the vein valve are assigned different elastic properties as detailed later.

At the beginning of the simulation, when the system is unperturbed, we establish contacts between nodes in the valve lattices and nodes in the vein wall lattice. In particular, nodes in the valve lattice which overlap the vein wall are considered to be dependent on the vein wall lattice. These dependent nodes obtain their displacements from the displacements of the vein wall lattice nodes, and the forces exerted on these dependent nodes are applied directly to the vein wall lattice nodes.

It should be noted that the sinus regions of the vein are more distensible than other regions of the vein wall. Furthermore, the valve structure is likely to be more flexible and thinner in the centre of the vein than where the valve attaches to the

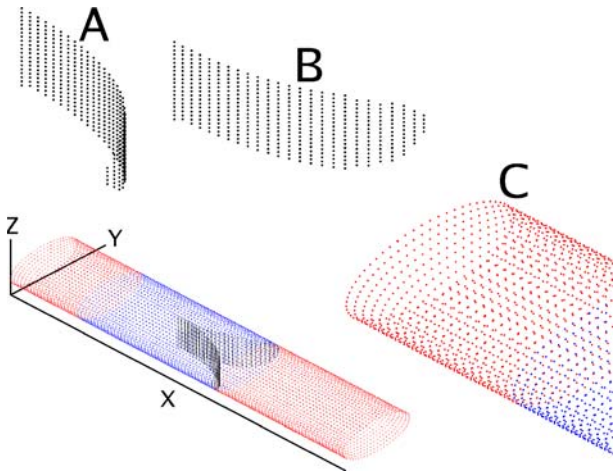

Fig. 1 LSM lattice structure of both vein leaflets (**a** and **b**) and vein wall (**c**). For clarity the LSM lattice is shown both separately and collectively

vein wall. We take this heterogeneity into consideration in our LSM model by locally varying the elastic spring constant. The local reduction in Young's modulus has been mentioned in experimental papers, but no quantitative information is obtainable. The form chosen here simply allows the sinus region to expand as observed experimentally. In particular, the sinus region is considered to be between $x = 4$ cm and $x = 6$ cm (a sinus depth of 2 cm) and the force constant between $x = 2$ cm and $x = 6$ cm is chosen in order to qualitatively mimic experimental observations [11]

$$k = \begin{cases} k_0(0.05 + 0.105(x-5)^2) & (x < 5) \\ k_0(0.05 + 0.95(x-5)^2) & (x > 5) \end{cases} \tag{6}$$

where x is the distance along the length of the vein and the spring constant is locally reduced to 5% of its normal value. The stiffness of the valve leaflet is reduced as a function of the initial radial distance R. The stiffness is given by $k = k_0(0.9\frac{R}{R_0} + 0.1)$, where R_0 is the radius of the vein. Therefore, the stiffness of the valve is reduced to 10% at the centre of the vein channel ($R = 0$).

We now turn our attention to the calculation of the hydrodynamics, and the fluid pressures which act upon this solid structure.

2.2 Fluid Dynamics

In the current study we use the lattice Boltzmann (LB) method [13] to solve the hydrodynamics of blood flow. The LB method is chosen as it has been used previously to capture both blood flow [17–20] and fluid–structure interactions [21–26]. Only a brief description of the LB method is given here and the reader is referred to the works of Verberg and Ladd [27, 28], Frisch et al. [29], He and Luo [30, 31], and d'Humières et al. [32] for a more complete description.

The LB model consists of a particle distribution function which evolves according to the following equation

$$f_i(\mathbf{r} + \mathbf{e}_i\Delta t, t + \Delta t) = f_i^{\star}(\mathbf{r}, t) = f_i(\mathbf{r}, t) + \Omega_i[\mathbf{f}(\mathbf{r}, t)] \tag{7}$$

where $f_i(\mathbf{r}, t)$ represents the density of fluid particles at position $\mathbf{r}$, time t, and with a velocity $\mathbf{e}_i$ [29]. Similar to real fluids on the microscopic scale, the LB model

evolves through both the propagation, and subsequent collision, of fluid particles. The collision of the fluid particles is illustrated in the above equation through the inclusion of the post-collision term, $f_i^\star(\mathbf{r}, t)$. The propagation is assumed to occur on the confines of the lattice. The collision operator, $\Omega_i[\mathbf{f}(\mathbf{r}, t)]$, relaxes the stresses toward local equilibrium and accounts for instantaneous collisions between fluid particles at the lattice nodes [28].

There are 19 fluid velocities in the three-dimensional model used here (referred to as D3Q19) which correspond to a rest velocity ($\mathbf{e} = [000]$) and velocities in the nearest- ($\mathbf{e} = \{100\}$) and next-nearest-neighbour ($\mathbf{e} = \{110\}$) directions.

The velocity moments of the particle distribution function are the hydrodynamic quantities, mass density ρ, momentum density $\mathbf{j}$, and the momentum flux Π. These are given by

$$\begin{aligned} \rho &= \sum_i f_i \\ \mathbf{j} &= \sum_i f_i \mathbf{e}_i = \rho \mathbf{v} \\ \Pi &= \sum_i f_i \mathbf{e}_i \mathbf{e}_i \end{aligned} \tag{8}$$

where $\mathbf{v}$ is the fluid velocity.

The boundaries are included using a non-slip link bounce-back scheme [28]. This scheme takes a particle distribution as it streams towards a wall node and bounces it back to the node it came from. For stationary walls, this is described by the propagation step $f_k(\mathbf{r}, t + \Delta t) = f_i^\star(\mathbf{r}, t)$, where k represents the direction opposite to the i direction; further details regarding the bounce-back scheme can be found in the next section. At the inlet and outlet of the system we assign constant pressure boundary conditions and put the gradient of the velocity to zero. In other words, we assign equilibrium distribution functions at the boundary nodes with a predetermined boundary density and velocities which are obtained from LB sites one lattice spacing in from the boundary nodes. We have shown how the LSM can simulate the elastic mechanics of the vein valve, and the LB can capture venous hemodynamics. We now detail the solid-fluid coupling between these two systems.

2.3 Coupling Fluid and Solid Models

In order for the vein walls and fluid to interact, the fluid must impose pressures and viscous stresses on the solid walls, whilst at the same time the fluid velocity at the walls must be equal to the velocity of the walls. A simple two-dimensional diagram of the fluid structure interface is given in Fig. 2. The LSM springs and nodes are not fixed in space and can freely move (as the structure deforms). However, the LB lattice is fixed and the discrete solid-fluid interface is defined by the regions where the LB links cross the LSM lattice; the method of establishing whether or not a LB link crosses a two-dimensional ‘tile’ is given in the Appendix. The LB lattice consists of nodes which are considered fluid and nodes which are considered solid. These definitions are transient, and change as the LSM structure moves with respect to the underlying LB lattice. It is, therefore, necessary to identify which LB nodes are fluid and which are solid.

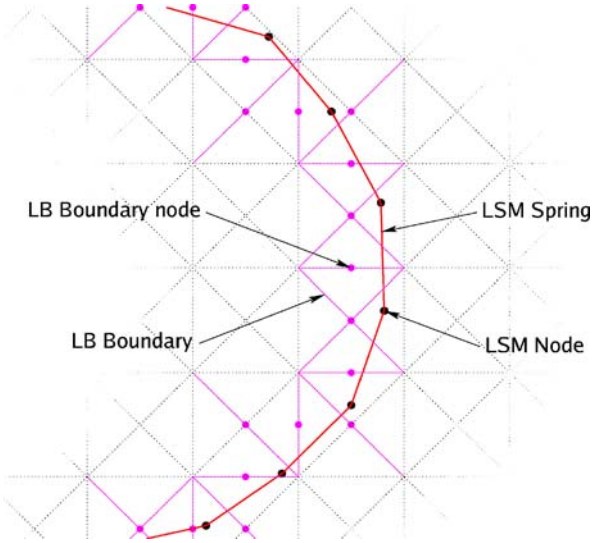

Fig. 2 Simple two-dimensional representation of the fluid–structure interaction. The *LSM lattice changes shape* as the solid structure becomes deformed. The *LB lattice remains fixed* and the fluid–solid interface in the LB model is given by the LB boundary links

We first obtain the LB boundary links on the LB lattice, which are defined as links which cross the LSM lattice structure. In the case of the vein walls, these represent the interface between fluid LB nodes and solid LB nodes. Once these boundary links are obtained, we can perform a cluster-counting operation to find regions within the vein walls (fluid LB nodes) and regions outside of the vein wall (solid LB nodes). In particular, by defining clusters as collections of LB nodes which do not cross LB boundary links, a simple cluster-counting algorithm will produce two clusters, one inside the vein walls and one outside. However, not all boundary links separate fluid and solid regions. The boundary links for the valve structure separate fluid regions on one side of the valve structure from fluid regions on the other side. These boundary links, however, do not contribute towards the cluster-counting procedure.

Once the fluid domain is identified (as the region of fluid LB nodes inside the vein) we can evolve the LB model for the fluid dynamics. The velocity of the surrounding solid walls, and the internal walls of the vein structure, influence the no-slip boundary conditions for the fluid. In particular, fluid particles that are being streamed towards a boundary node are reflected back in the direction they came from in the following manner [28],

$$f_k(\mathbf{r}, t + \Delta t) = f_i^{\star}(\mathbf{r}, t) - \frac{2\rho a_i \mathbf{e}_i \cdot \mathbf{v}_b(\mathbf{r}_b)}{c_f^2} \tag{9}$$

where k indicates the direction opposite to i, and $\mathbf{v}_b$ is the velocity at the boundary node, situated at $\mathbf{r}_b = \mathbf{r} + \mathbf{e}_i/2$. This link bounce-back scheme ensures that the velocity of the fluid follows the velocity of the wall, and that mass is conserved. The velocity at the LB boundary node can be obtained from the velocity of the neighbouring LSM nodes. In particular, we perform a weighted average of the velocities at the surrounding LSM nodes, where the velocities are weighted by

the inverse of the distance from LB boundary node to LSM node, squared [21]. The velocity of the LB boundary node is of the form,

$$\mathbf{v}_b(\mathbf{r}_b) = \frac{\sum_{\mathbf{r}} \left[\mathbf{v}(\mathbf{r})/(\mathbf{r}-\mathbf{r}_b)^2\right]}{\sum_{\mathbf{r}} \left[1/(\mathbf{r}-\mathbf{r}_b)^2\right]} \tag{10}$$

where $\mathbf{r}$ and $\mathbf{v}(\mathbf{r}_b)$ are the position and velocity of neighbouring LSM nodes. The summation is taken over all the LSM nodes within a given distance. This provides an efficient way of transferring the velocity from the LSM lattice to the LB boundary nodes.

In the link bounce-back boundary scheme, as just mentioned, fluid propagating towards the boundary is reflected back at the LB boundary nodes. Therefore, there is a change in momentum occurring at the boundary, which results in a fluid pressure which acts on the solid wall. This force, located at the LB boundary nodes, is given by [28]

$$\mathbf{F}_b\left(\mathbf{r}_b, t+\frac{\Delta t}{2}\right) = 2\left(f_i^{\star}(\mathbf{r},t) - \frac{2\rho a_i \mathbf{e}_i \cdot \mathbf{v}_b(\mathbf{r}_b)}{c_f^2}\right)\mathbf{e}_i \tag{11}$$

where, in the current paper, we subtract an additional amount of $2\rho_0 a_i \mathbf{e}_i$ to account for an external density ρ_0. In real systems, the external environment is expected to be more complicated than what we consider here and it is unclear what effect this surrounding tissue might have on the function of a vein valve. The fluid pressure, however, is located on the LB lattice and must be distributed to the solid LSM lattice. In a similar manner to how we transfer the velocity of the LSM nodes to the LB lattice, we can distribute the forces from the LB lattice to nearby LSM nodes. In particular, we again weight the distribution of the forces by the inverse of the distance from LSM node to LB boundary node, squared [21]. The force acting on a solid LSM node, from the fluid pressure, is given by

$$\mathbf{F}(\mathbf{r}) = \sum_{\mathbf{r}_b} \mathbf{F}_b(\mathbf{r}_b) \frac{1/(\mathbf{r}-\mathbf{r}_b)^2}{\sum_{\mathbf{r}} 1/(\mathbf{r}-\mathbf{r}_b)^2}. \tag{12}$$

In this manner, we ensure that the forces acting on the solid boundary wall are efficiently distributed to the solid LSM nodes. The velocities of the LSM nodes are also efficiently conveyed to the boundary in the LB fluid, enabling us to capture the dynamic fluid–structure interactions in the vein valve system.

3 Results

We investigate the fluid–structure interactions that act between the vein valve mechanical structure and the venous hemodynamics. In particular, we apply a pressure gradient across the system and simultaneously evolve the solid mechanics and fluid hydrodynamics towards equilibrium. The vein wall is considered to have a Young's modulus of 1,000 kN m^{-2} [5, 33] and a thickness of 0.05 cm. The density of blood is taken to be 1,060 kg m^{-3} and the blood viscosity to be 0.0027 Ns m^{-2} [34]. The response of the vein valve structure to a pressure difference of 13.8 kPa (proximal to distal) is shown in Fig. 3. For clarity, only half of the vein wall is shown and the cusps of the vein valve are coloured grey. The pressure difference pushes the valve

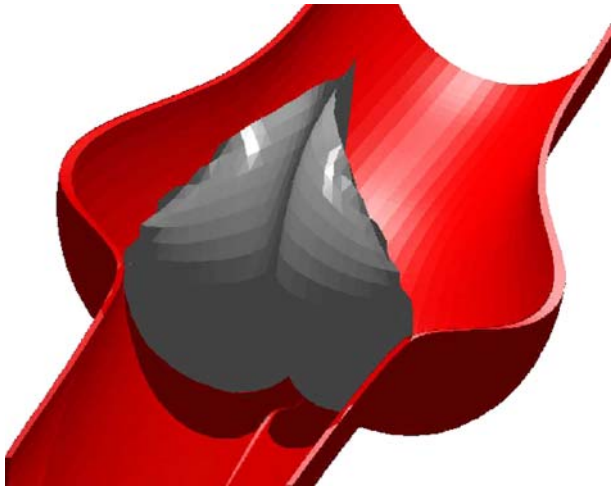

Fig. 3 Response of the vein valve to a (proximal to distal) pressure difference of 13.8 kPa. The vein leaflets (*coloured grey*) remain closed, occluding the vessel and restricting retrograde blood flow

cusps together, occluding the flow of blood, and 'inflates' the valves. Furthermore, the fluid pressure causes the valve sinuses to 'balloon' out. It should be noted that the vein wall near the sinus becomes inflated as the Young's modulus of the wall in this region is reduced. In particular, the deformation in Figs. 3 and 4 can be compared with Fig. 1 which shows the region of reduced Young's moduli. The response of the vein valve, to a proximal to distal pressure difference, is to ensure that the valve is closed and retrograde blood flow is prevented. However, a distal-to-proximal pressure difference has the opposite effect.

Figure 4 shows the same structure as shown in Fig. 3, but in response to a distal-to-proximal pressure difference of 13.8 kPa. Here the fluid pressure pushes the valve cusps away from each other and results in an opening in the centre of the vein. In particular, the valve cusps remain attached to the vein wall but no longer

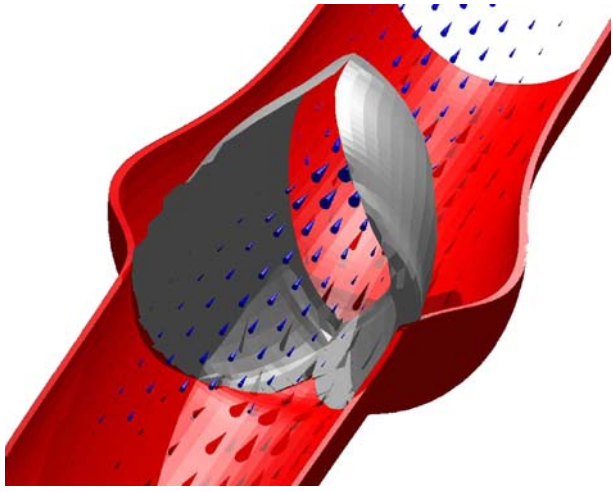

Fig. 4 Response of the vein valve to a (distal to proximal) pressure difference of 13.8 kPa. The pressure pushes the valve open, allowing blood to stream through the open valve (*blood flow is indicated by the cones*)

meet or overlap in the centre of the vein. The pressure forces the valve cusps to move away from the centre of the vein, and towards the vein wall, opening the vein valve. Blood can, therefore, flow proximally through the open vein valve; the velocity and directionality of this blood flow is indicated by the blue cones in Fig. 4. It should be noted, however, that we do not observe the valve leaflet 'fluttering,' as observed experimentally, and this may be due to the damping in the LSM solid or our assumption of a homogeneous Newtonian fluid.

The flow field in the same system depicted in Fig. 4 is plotted in Fig. 5a, which shows the fluid flow in the central plane, i.e., the plane which passes through both the valve sinuses and vein opening area. The magnitude of the flow is indicated by the contours (black indicates zero velocity and white a velocity of 36 cm s^{-1}). The magnitude and direction of the fluid flow is also indicated by the size and orientation of the arrows. Blood flows through the open valve and the velocity of the blood flow is greatest as it passes through the vein valve opening. The velocity is also higher in the centre of the channel than at the walls where no-slip boundary conditions are enforced. Figure 5b shows a close up of this flow field, at a region where the fluid flows back behind the valve cusp and into the valve sinus. Note that the axes on Fig. 5b run from $x = 3.8$ to $x = 4.2$ and $y = 0.8$ to $y = 1.2$ and that this is an enlargement

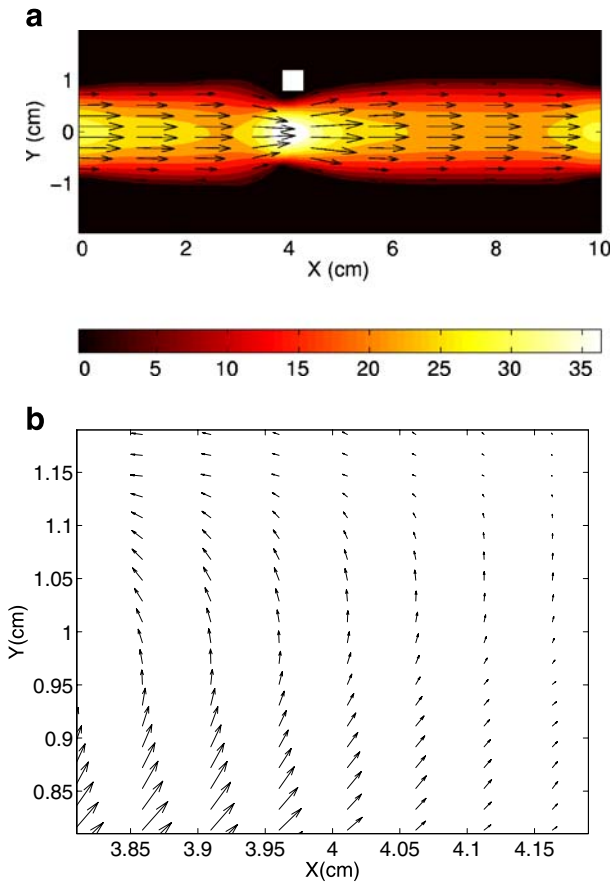

Fig. 5 Two-dimensional velocity profile through the *centre* of the simulation. The system has a distal-to-proximal pressure difference of 13.8 kPa. In (**a**) the magnitude of the velocity is indicated by the *contours* (in units of cm s^{-1}), and the magnitude and directionality of flow is indicated by the *arrows*. In (**b**), we present a close-up view of the velocity profile in the small square region in (**a**), showing vortical flow in the valve sinus pocket

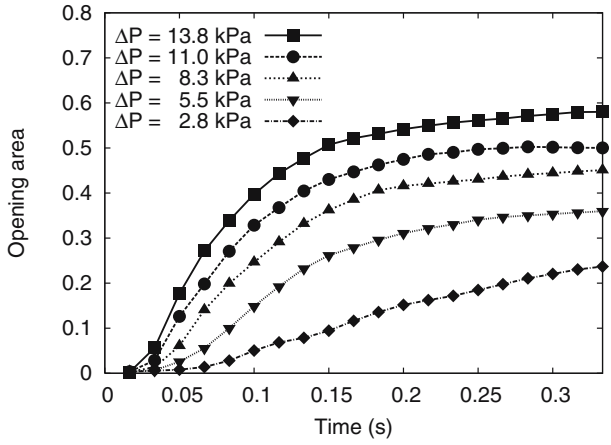

Fig. 6 Opening area of the valve (divided by the cross-sectional area of the undeformed vein tube) as a function of time. Systems with different pressure differences are contrasted

of the region indicated by the small white square in Fig. 5a, which shows the full system. At the region of the vein valve where the faster moving fluid through the open valve meets the slower moving fluid in the wider vein channel, some of the blood is redirected into the valve sinus. This results in a recirculation of the blood in the valve sinus and such flow is thought to prevent stasis inside the valve pocket [12].

In order to quantify the dynamics of vein valve opening, in Fig. 6, we show the ratio of the opening area to the undeformed vein cross-sectional area as a function of time for various distal-to-proximal pressure differences. The vein valve is initially closed at time $t = 0$, and the difference in pressure forces the valve open. The valve opens reasonably quickly before the valve opening area plateaus at an equilibrium value. As the pressure difference is reduced, the valve opening area is also reduced. Furthermore, it appears to take a longer time for the structure to evolve towards an equilibrium state (the vein opening area takes longer to plateau) in systems with lower pressure differences.

Not only can we measure the area of the valve that is open, but also the flow rate of blood through this opening. In Fig. 7, we show the corresponding blood flow

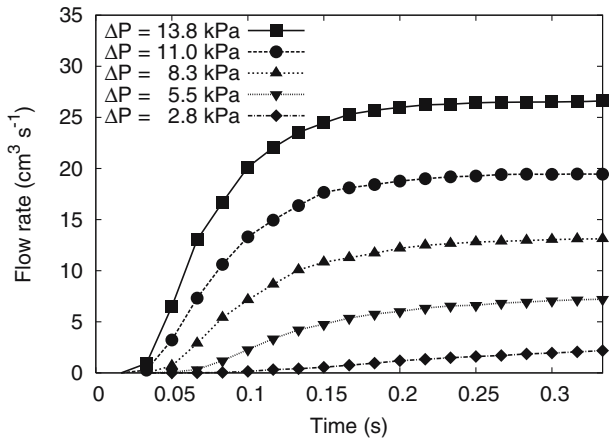

Fig. 7 Flow rate of blood through the valve as a function of time. Systems with different pressure differences are contrasted

rates as a function of time for systems of varying pressure difference. The flow rate also suddenly increases and plateaus as a function of time, in a similar manner as the valve opening area. The flow rate, however, plateaus at a value which is more sensitive to the pressure difference. That is, the pressure difference not only forces the valve open but is also the driving force for fluid flow through the valve. Reducing the pressure difference results in a smaller valve opening for the fluid to pass through and reduces the driving force for fluid flow through the aperture. Therefore, the flow rate through the valve is significantly reduced.

4 Summary and Conclusions

To summarise, we have developed an efficient[1] computer model which captures the dynamics of a vein valve. We couple the solid mechanics of both the vein wall, and the valve leaflets, with the hydrodynamics of the blood flow. Our model captures the essential features of vein valve mechanics, allows us to visualise and quantify the vein valve hemodynamics, and reveals interesting insights into the structural dynamics of these complex systems. In particular, these simulation results illustrate the basic physics of vain valves: restricting the retrograde flow of blood and ensuring unidirectional blood flow through the vein valve.

It should be noted that the model presented in this paper only gives a qualitative description of a vein valve. There are many areas of improvement which might help to make this model more quantitative, including (1) the incorporation of nonlinear elasticity for the vein walls and surrounding tissue, (2) the extension of the fluid to include non-Newtonian fluid dynamics, and (3) a more accurate physiological description of the geometry and local stiffnesses of the vein and valves. To our knowledge, however, this is the first computer simulation of a vein valve and the coupling of fluid and structure in these systems represents a significant advancement in this field. Future work, therefore, will seek to address some of these issues, and, through collaboration with experimental groups, we hope to obtain the physiological information, required for parameterising these computer simulations.

Future work will also concentrate on applying this model to dysfunctional vein valves. In particular, we can systematically increase the spring lengths in the LSM of the vein wall and simulate venous dilation. Alternatively, we can shorten or remove springs from the LSM of the vein valve and elucidate the effects of valve shrinkage or damage. In this manner, we can gain crucial insights into various forms of venous dysfunction and help predict possible treatments for these disorders.

Appendix

In order to identify fluid and solid regions in the LB model, and locate the LB boundary nodes, we must determine when a LB link crosses a LSM 'tile', which is defined as the area between neighbouring LSM nodes, e.g., between nodes at positions $\mathbf{r}(i, j)$, $\mathbf{r}(i+1, j)$, $\mathbf{r}(i, j+1)$ and $\mathbf{r}(i+1, j+1)$. The cylindrical vein wall is

[1] An average simulation takes roughly seven hours on a standard Linux machine with a 3GHz Xeon processor.

described, in a sense, by these LSM tiles and determining if a LB link crosses these tiles can tell us which LB links straddle the fluid-solid boundary. Furthermore, it is necessary to determine which LB links cross the LSM tiles which make up the valve cusps in order to ensure that the fluid–structure interactions are accounted for in these regions. A LSM tile is shown in Fig. 8, consisting of four corner points (A, B, C, and D). We can spatially interpolate any point between these corner points using the two variables s and t. Furthermore, the LB link is shown as a line in Fig. 8 and a point on this line is mathematically described as $\mathbf{L} + u\Delta\mathbf{L}$ where $\mathbf{L}$ is the location of a LB node, u is a variable between 0 and 1, and $\Delta\mathbf{L}$ is a vector to a neighbouring node. If the LB link crosses the LSM tile, then the following equation is satisfied

$$\mathbf{L} + u\Delta\mathbf{L} = (1-s)(1-t)\mathbf{C} + s(1-t)\mathbf{A} + t(1-s)\mathbf{D} + st\mathbf{B} \tag{13}$$

for values of u, s and t between 0 and 1. As an example, we consider LB links of the form, $\Delta\mathbf{L} = [100]$. We obtain the following equations

$$u = (1-s)(1-t)C_x + s(1-t)A_x + t(1-s)D_x + stB_x - L_x \tag{14}$$

$$s = \frac{L_y - (1-t)C_y - tD_y}{(1-t)(A_y - C_y) + t(B_y - D_y)} = \frac{L_z - (1-t)C_z - tD_z}{(1-t)(A_z - C_z) + t(B_z - D_z)} \tag{15}$$

$$\begin{aligned} 0 = {} & (L_y - C_y)(A_z - C_z) - (L_z - C_z)(A_y - C_y) \\ & + t\big[(C_y - D_y)(A_z - C_z) - (C_z - D_z)(A_y - C_y) + (B_z - D_z - A_z + C_z) \\ & \quad \times (L_y - C_y) - (B_y - D_y - A_y + C_y)(L_z - C_z)\big] \\ & + t^2\big[(c_y - D_y)(B_z - D_z - A_z + C_z) - (C_z - D_z)(B_y - D_y - A_y + C_y)\big] \end{aligned} \tag{16}$$

We obtain two values of t from the quadratic (16). If either of the values are between 0 and 1 then we can substitute this value into (15) to obtain a value of s. If this yields

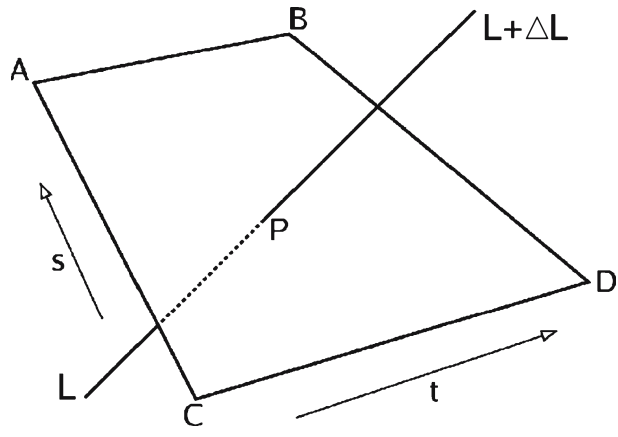

Fig. 8 Intersection of a line (LB link) with a 'tile' (area between neighbouring nodes of a LSM lattice)

a value of s between 0 and 1, we can substitute this value, and the t value, into (14) to obtain a value for u. If the value for u is also between 0 and 1, then the LB link crosses the LSM tile.

References

1. Vander, A., Sherman, J., Luciano, D.: Human Physiology, 7th edn. McGraw-Hill, New York (1998)
2. Sherwood, L.: Human Physiology. Thomson Learning, London (2004)
3. Patton, T.: The Human Body in Health and Disease. Elsevier, Holland (2005)
4. Notowitz, L.B.: Normal venous anatomy and physiology of the lower extremity. J. Vasc. Nurs. **11**, 39–42 (1993)
5. Buescher, C.D., Nachiappan, B., Brumbaugh, J.M., Hoo, K.A., Janssen, H.F.: Experimental studies of the effects of abnormal venous valves on fluid flow. Biotechnol. Prog. **21**, 938–945 (2005)
6. Ono, T., Bergan, J.J., Schmid-Schonbein, G.W., Takase, S.: Monocyte infiltration into venous valves. J. Vasc. Surg. **27**, 158–166 (1998)
7. Ackroyd, J.S., Pattison, M., Browse, N.L.: A study of the mechanical properties of fresh and preserved human femoral vein wall and valve cusps. Br. J. Surg. **72**, 117–119 (1985)
8. van Bemmelen, P.S., Beach, K., Bedford, G., Strandness, D.E.: The mechanism of venous valve closure. Arch. Surg. **125**, 617–619 (1990)
9. Qui, Y., Quijano, R.C., Wang, S.K., Hwang, N.H.C.: Fluid dynamics of venous valve closure. Ann. Biomed. Eng. **23**, 750–759 (1995)
10. Lurie, F., Kistner, R.L., Eklof, B.: The mechanism of venuous valve closure in normal physiologic conditions. J. Vasc. Surg. **35**, 713–717 (2002)
11. Lurie, F., Kistner, R.L., Eklof, B., Kessler, D.: Mechanism of venous valve closure and role of the valve in circulation: a new concept. J. Vasc. Surg. **38**, 955–961 (2003)
12. Lurie, F., Kistner, R.L., Eklof, B., Kessler, D.: A new concept of the mechanism of venous valve closure and role of valves in circulation. Phlebology **13**, 3–5 (2006)
13. Chen, S., Doolen, G.D.: Lattice Boltzmann method for fluid flows. Annu. Rev. Fluid Mech. **30**, 329–364 (1998)
14. Buxton, G.A., Care, C.M., Cleaver, D.J.: A lattice spring model of heterogeneous materials with plasticity. Model. Simul. Mater. Sci. Eng. **9**, 485–497 (2001) and references therein
15. Monette, L., Anderson, M.P.: Elastic and fracture properties of the 2-dimensional triangular and square lattices. Model. Simul. Mater. Sci. Eng. **2**, 53–66 (1994)
16. Tuckerman, M., Berne, B.J., Martyna, G.J.: Reversible multiple time scale molecular-dynamics. J. Chem. Phys. **97**, 1990 (1992)
17. Krafczyk, M., Cerrolaza, M., Schulz, M., Rank, E.: Analysis of 3D transient blood flow passing through an artificial aortic valve by lattice-Boltzmann methods. J. Biomech. **31**, 453–462 (1998)
18. Dupin, M.M., Halliday, I., Care, C.M.: Multi-component lattice Boltzmann equation for mesoscale blood flow. J. Phys. A **36**, 8517 (2003)
19. Dupin, M.M., Halliday, I., Care, C.M.: A multi-component lattice Boltzmann scheme: towards the mesoscale simulation of blood flow. Med. Eng. Phys. **8**, 13–18 (2006)
20. Boyd, J., Buick, J., Cosgrove, J.A., Stansell, P.: Application of the lattice Boltzmann model to simulated stenosis growth in a two-dimensional carotid artery. Phys. Med. Biol. **50**, 4783–4796 (2005)
21. Buxton, G.A., Verberg, R., Jasnow, D., Balazs, A.C.: Newtonian fluid meets an elastic solid: coupling lattice Boltzmann and lattice spring models. Phys. Rev. E **71**, 056707 (2005)
22. Balazs, A.C.: Challenges in polymer science: controlling vesicle-substrate interactions. J. Polym. Sci. Part B, Polym. Phys. **43**, 3357–3360 (2005)
23. Alexeev, A., Verberg, R., Balazs, A.C.: Modeling the motion of microcapsules on compliant polymeric surfaces. Macromolecules **38**, 10244–10260 (2005)
24. Alexeev, A., Verberg, R., Balazs, A.C.: Designing compliant substrates to regulate the motion of vesicles. Phys. Rev. Lett. **96**, 148103 (2006)
25. Alexeev, A., Verberg, R., Balazs, A.C.: Modeling the interactions between deformable capsules rolling on a compliant surface. Soft Matter **2**, 499–509 (2006)
26. Smith, K.A., Alexeev, A., Verberg, R., Balazs, A.C.: Designing a simple ratcheting system to sort microcapsules by mechanical properties. Langmuir **22**, 6739–6742 (2006)

27. Verberg, R., Ladd, A.J.C.: Simulation of chemical erosion in rough fractures. Phys. Rev. E **65**, 056311 (2002)
28. Ladd, A.J.C., Verberg, R.: Lattice-Boltzmann simulations of particle-fluid suspensions. J. Stat. Phys. **104**, 1191 (2001) and references therein
29. Frisch, U., d'Humières, D., Hasslacher, B., Lallemand, P., Pomeau, Y., Rivet, J.-P.: Lattice gas hydrodynamics in two and three dimensions. Complex Syst. **1**, 649 (1987)
30. He, X., Luo, L.-S.: A priori derivation of the lattice Boltzmann equation. Phys. Rev. E **55**, R6333 (1997)
31. He, X., Luo, L.-S.: Theory of the lattice Boltzmann method: from the Boltzmann equation to the lattice Boltzmann equation. Phys. Rev. E **56**, 6811 (1997)
32. d'Humières, D., Ginzburg, I., Krafczyk, M., Lallemand, P., Luo, L.-S.: Multiple-relaxation-time lattice Boltzmann models in three dimensions. Philos. Trans. R. Soc. London, Ser. A **360**, 437 (2002)
33. Wesly, R.L., Vaishnav, R.N., Fuchs, J.C., Patel, D.J., Greenfield, J.C.: Static linear and nonlinear elastic properties of normal and arterialized venous tissue in dogs and man. Circ. Res. **37**, 509 (1975)
34. Guyton, A.C., Hall, J.E.: Textbook of Medical Physiology. Elsevier, Philadelphia (1996)